Contrastive Analysis on the Property of Solar Air Collectors with Different Surface Shapes

Shuilian Li 1, Dapeng Yang1, Xinli Wei2*

¹School of Architecture and Environmental Engineering, Zhengzhou Technical College, Zhengzhou, Henan, China

²Zhengzhou University, Zhengzhou, Henan, China

*Corresponding Author.

Abstract

Addressing the issue of low efficiency of flat plate collectors, the purpose of this article is to offer remedial measures about the problem of low absorptivity of absorption plates. In the study, three types of absorption plates were analyzed, type-I is the basic flat plate, type-II is the V-shaped plate, and type-III is the sinusoidal corrugated absorption plate. Experimental research and simulation were conducted on light path on the absorption plate with them. The results indicate that the heat exchange area of the sinusoida-corrugated plate is the largest, which is 3.86 times of that of flat plate, the air temperature rise of the sinusoida-corrugated plate is the tallest among the three types under the same external environment, which is 7.66°C than that of the type-I, and type-III has also the highest absorption rate, increasing by 10.78 % higher than that of flat plate. This can provide reference for studying the performance of different collector plates.

Keywords: Solar energy; air collector; absorption rate; optical path

1. Introduction

Solar collectors give play to a crucial function in the utilization of solar energy systems. Solar collectors are divided by the fluid into solar hot water collectors and solar air collectors. Even though the efficiency of SAHC is low due to the poor thermodynamic properties of air in heat interchange in contrast to liquids, it is yet extensive used worldwide due to its advantages such as easy structure and so on. So as to enhance the heat transfer coefficient, lots of advanced technologies have been built and exploited. One technology is to alter the surface profile of the absorber. In the design of solar air collectors, the surface shape factor of the absorber is the uppermost arguments. In an effort to capture the entire spectrum of solar radiation, it is supposed to selectivity, with high absorption and low reflectivity of solar radiation. The influence of the structure and material of the absorption plate on the efficiency of the collector has been extensively discussed in the papers.

In recent years, many researchers have conducted extensive thermodynamic analysis and research on solar collector systems. Yemeli Wenceslas Koholé et al. [1] studied using exergy analysis and numerical simulation to study the thermal performance and optimized operation of flat panel solar collectors. Kumar R. [2] designed and fabricated a combination of concave and convex roughness elements on the absorption plate. Varun Goel et al. [3] conducted overview of the development and application of solar air heaters. Aman Soi [4] made to review the geometric shapes of pits and protrusions used in SAHs pipelines, as well as the correlations between Nusselt numbers and friction coefficients developed by various researchers. Anil Kumar et al. [5] studied summary of exergy analysis of solar parabolic heat collectors. Navneet Arya [6] conducted a solar air heater that combines V-shaped, curved, and transverse fractured micro with pits on the absorber panel to better heat transfer. Alok Dhaundiyal [7] investigated comprehensive analysis of natural ventilation solar driers. Selçuk Darici [8] studied the properties of solar air collectors having trapezoidal corrugated and flat absorber plates. Abdulmohsen O. Alsaiari [9] reseached heat transfer and airflow friction in solar air heaters with ribbed absorption plates. Yan

Volume 18, No. 3, 2024

ISSN: 1750-9548

Jiang et al.[10] proposed a new solar air collector having a tilted transparent cover plate. Hirofumi Hattori [11] assigned characteristics and structure of thermal stratified turbulent boundary layer. Hüseyin Benli [12] conducted experimental research on the configuration and permutation of the collector to offer a better heat transfer surface. Alsaleem S. M. [13] studied the effect of rib wall number on the thermal performance of 45° parallel or cross ribbed rectangular channels. Gargioni G. T. [14] enhanced heat transfer in the flow of a triangular turbulent promoter in a closed channel. Natural convection heat transfer in ribbed vertical plates were discussed by Giovanni Tanda et al. [15]. Wang C. S. et al. [16] evaluated the effects of multi hole and stream ripple on the thermal performance of microchannels using a new approach. Mahfuzur Rahman [17] also studied numerical and benchmark testing of bilateral rib roughening, bilateral heat transfer, and pressure loss characteristics in narrow rectangular channels. Hui Xiao [18] discussed heat transfer performance and flow properties of a solar air heater using a trapezoidal vortex generator. Jacek Kasperski [19] investigated the thermotechnical performance of a centralized solar air heater with an internal multi fin array. Kushagra S. [20] conducted heat transfer and fluid flow analysis on solar air heater. Li shuilian [21] studied the influence of buoyancy on the property of solar air collectors with distinct constructions, and so on.

However, the current research is only conducted from the perspective of heat transfer, and rarely from the perspective of optics. This paper designs and builds three different structures of solar air collectors. A comparative study was conducted on their performance from both optical and thermal perspectives, providing a reference for studying the effect of plate shape on heat transfer in solar collectors

2. Material and Methods

2.1 Experimental device

The schematic design and the experimental device of a solar air collector are shown in Figure 1, which consists of essentially the same components as traditional solar air collectors with flat plate, the solar air collectors tested for the experiments has a distinctive structure because of its absorbing surface. The solar air system is composed of an inlet, a testing area, an outlet, a flow meter, and a blower. The air passage is 1950 mm× 950 mm× 50 mm. The diameter of the inlet and outlet sections is 100 mm. As shown in the Figure 2, there are three different surface shapes of absorption plates. Type-I is a traditional flat-plate. Type-II is a V shape plate with an angle of 45 degrees. Type-III is a sinusoidal-corrugated absorption plate with the same size as other types. The wavelength of type-III is equal to twice the peak value, which is 40 mm. All absorption plates are made of aluminum plates with the same thickness of 2mm to obtain uniform radiation. The surface of the collector plate is evenly sprayed with blue paint to absorb solar radiation. To minimize heat loss to the greatest extent possible, all absorption plates are insulated with 50 mm thick glass wool at the bottom and sides. In this study, the experiments were conducted on the campus of Zhengzhou University in Zhengzhou city of China, which is located at 113.42°E and 34.44°N. As measured in summer, the absorber plate were placed facing south and tilting 25° relative to the horizontal line.

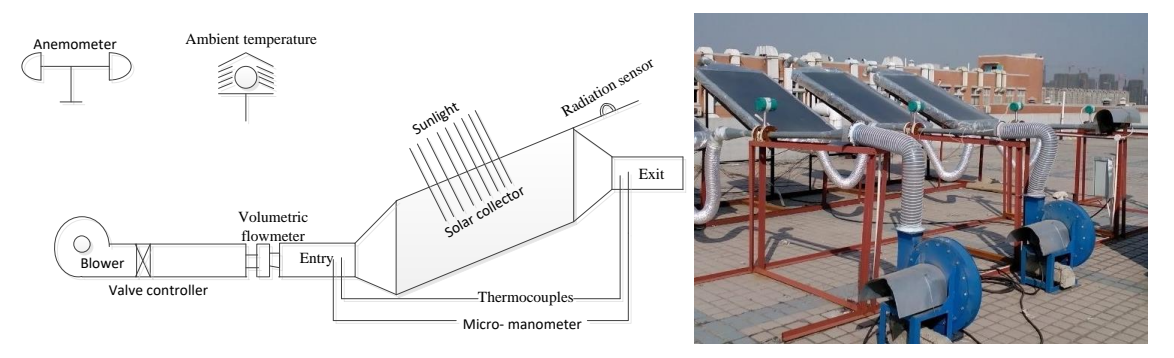


Figure 1 Schematic diagram and experimental setup of solar air collectors

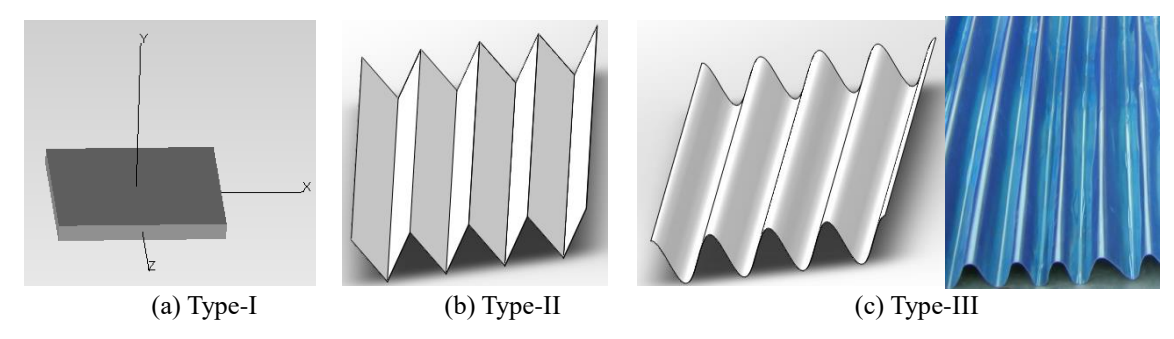


Figure 2 Absorber plates with different structure

2.2 Temperature measurement

The temperature of the absorption plate at different positions was measured using a thermal resistance Pt100 having precision of 0.1 °C and an Agilent data collection apparatus. Six thermal resistors were attached to the back of the absorption board to record the temperature of the board. The position of thermal resistance is shown in Figure 3. The heat resistance outcome is surveyed with the aid of Agilent data collection apparatus.

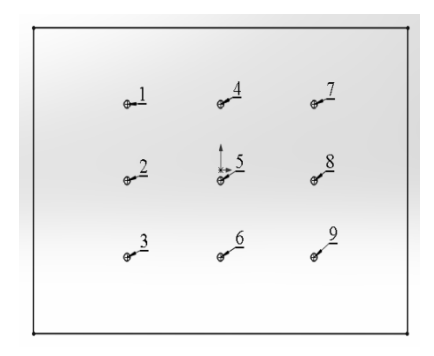


Figure 3 Location of thermal resistances on absorber plate

2.3 Radiant intensity measurement

Use the PHFSB radiation sensor to measure radiation intensity, which can be used to measure $0.3-3 \mu m$ spectral range of total solar radiation. Data can be achieved by connecting to a computer through a PH automatic weather station or directly reading from the computer, as shown in Figure 4.



(a) Radiation sensor (b) Automatic weather station (c) Agilent data collection apparatus (d) Computer

Figure 4 Experimental instruments

2.4 Experimental uncertainty

The nondeterminacy and mistake in tests may come from conditions, apparatus, circumstance, inspection, testing plan, and reading of instrument. Giving the relative uncertainty in a single factor represented by x_n , Les Kirkup [22] used the following equation to estimate the uncertainty. The probable errors in measurement in this survey were shown in Table 1.

$$w = \left[\left(x_1 \right)^2 + \left(x_2 \right)^2 + \left(x_3 \right)^2 \cdots \left(x_{n-1} \right)^2 + \left(x_n \right)^2 \right]^{\frac{1}{2}}$$
 (1)

Table 1 Uncertainty in parameter measurement process

Parameter	Unit	Comment
Temperature error		
Surface of absorber plate	$^{\circ}\mathrm{C}$	±0.15
Environment	$^{\circ}\mathrm{C}$	±0.15
Time error		
Temperature measurement	min	± 0.1
Solar radiation intensity error	\mathbf{W}	± 0.2
Reading error	%	±0.1

Within the whole experimental operating range, the uncertainty of Nusselt number is 5.03%, while the error in friction coefficient is approximately 3.04%.

3. Analysis

3.1 Theoretical derivation

As the temperature of the absorption plate increases, the instantaneous energy equation is satisfied, and its expression is as follows:

$$\alpha \cdot I \cdot A = \left(C_p M \left(\frac{dT}{dt}\right)_b + Q_{cond} + Q_{con} + Q_{ra}\right)$$
 (2)

In the formula, α is absorptivity of the absorption plate, I is the intensity of solar irradiance, A is the illumination area of the absorption plate. $(dT/dt)_h$ is the heating rate of the absorption plate, C_pM is the thermal capacity of the absorption plate, Q_{conv} , Q_{conv} , Q_{ra} are the heat exchange capacity between the absorption plate and the circumstance.

As the temperature of the absorption plate decreases, the instantaneous energy balance equation is achieved, and its expression is as follows:

$$-\left(C_{p}M\right)\left(\frac{dT}{dt}\right)_{c} = Q_{cond}^{'} + Q_{conv}^{'} + Q_{ra}^{'}$$
(3)

In the formula, $(dT/dt)_c$ is the rate of cooling for the absorption plate, and $Q_{cond}^{'}$, $Q_{conv}^{'}$, $Q_{ra}^{'}$ are the heat exchange capacity between the absorption plate placed in the louver box and the environment.

The heating and cooling process takes A very short period of time, and when the temperature is equal, the transient thermal state is the same. Therefore, the heating and cooling circumstance can be roughly considered the same. So we can suppose that at the same temperature, the instantaneous heat exchange of the absorption plate satisfies the following relationship:

$$Q_{cond} = Q_{conv}' \qquad Q_{conv} = Q_{conv}' \qquad Q_{ra} = Q_{ra}'$$
(4)

According to equations (1), (2), (3) and (4), α can be represented as follows:

$$\alpha = -\frac{C_{\rm p}M}{I \cdot A} [(dT/dt)_h - (dT/dt)_c]$$
 (5)

According to the heating and cooling curves of the absorption plate gained at the same T_0 temperature, the absorption rate of the absorption plate can be obtained by formula (5).

The performance evaluation of the collector in this experiment adopts the photothermal conversion efficiency of the air collector, which is defined as the ratio of the energy obtained from the heated air to the solar radiation energy incident on the surface of the collector. The expression is as follows:

$$\eta_a = \frac{{}_{ICP}(T_{a,out} - T_{a,in})}{I \cdot A}$$
(6)

3.2 Numerical simulation

TracePro is an optical simulation software mainly used in optical analysis systems, radiation analysis systems, lighting systems, and photometric analysis systems, using Monte Carlo Ray Tracing to track the path of light. This technology allows light to be imported into a built solid model, and at each physical surface or intersection, each beam of light follows the laws of reflection, absorption, scattering, and refraction. When light travels along different paths in a solid, TracePro can track the luminous flux of each ray and calculate the energy absorbed, refracted, specular reflected, and scattered by the light. Therefore, the light path on the absorption plate was simulated by TRACEPRO.

4. Results and Discussions

This article introduces and discusses the performance of solar air collectors with different structures. To conduct effectiveness testing of the collector, experimental data was collected on the same day and at the same time under the same radiation and clear sky conditions. To contrast the advantages and disadvantages of solar air collectors with sinusoidal corrugated collectors, ordinary flat collectors, and V-shaped collectors, a comparative analysis was conducted from three aspects: heat exchange area, optical path, and absorption rate.

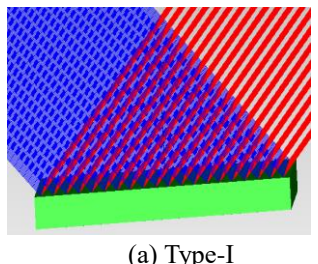
After calculation, the actual area of the flat plate can be obtained as: $1950 \times 950 = 1852500 \text{ mm}^2 = 1.85 \text{ m}^2$

The actual area of the V-shaped plate is: $20 / \sin 22.5^{\circ} \times 1950 \times 24 \times 2 = 4891771.74 \text{ mm}^2 = 4.89 \text{ m}^2$

The actual area of the sinusoidal-corrugated plate is: $1.91 \times 20 \times 1950 \times 24 \times 4 = 7151040 \text{ mm}^2 = 7.15 \text{ m}^2$

From the comparison, it can be seen that the area of the V-shaped collector plate is 2.64 times that of the flat plate, while the area of the sinusoidal corrugated collector plate is 3.86 times that of the flat plate. From this, it can be seen that in terms of heat exchange area, the sinusoidal corrugated collector plate has the largest area.

Figure 5 shows the optical path shinning on the absorber plate with different structures. In Figure 5, the color of the light represents the energy of the light, and the red represents the incident light, with the strongest energy. It can be seen from the Figure 5 that part of the light is absorbed by the surface coating of the collector plate, the rest is reflected out (blue part in the figure). when light shines on the flat absorber plate, the absorption and reflection of light only occur once, , while when light shines on the V shape plate and sinusoidal-corrugated plate, it occurs at least twice. And the distribution of light intensity with different absorbers is shown in Figure 6. As shown in the Figure 6, the total flux of Type-I is 109.95 W and the incident rays is 200, the light does not undergo secondary reflection and absorption. The total flux of Type-II is 240 W and the incident rays is 400, the total flux of Type-III is 300 W and the incident rays is 680, so the light is reflected and absorbed for many times. Type-III has more reflections and absorption times than Type-II.



(a) Type-I

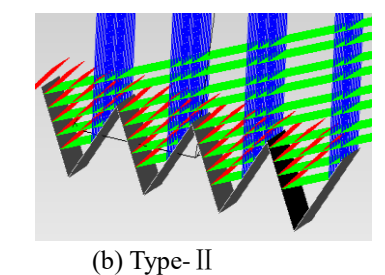
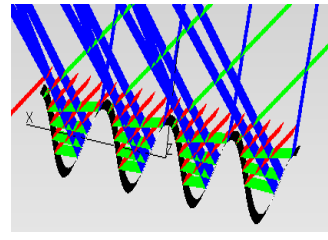


Figure 5 Light path of different plates



(c)Type-III

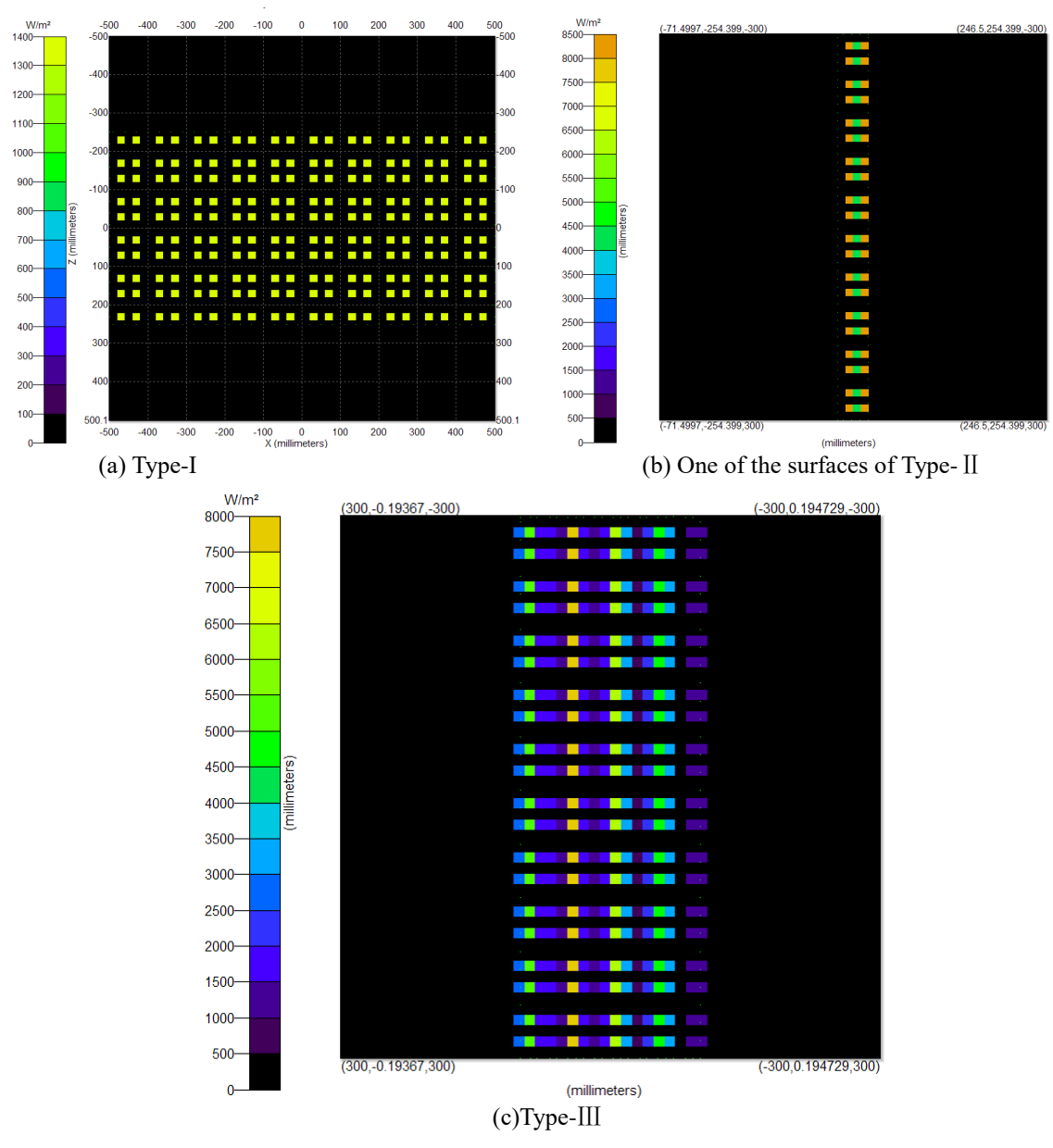


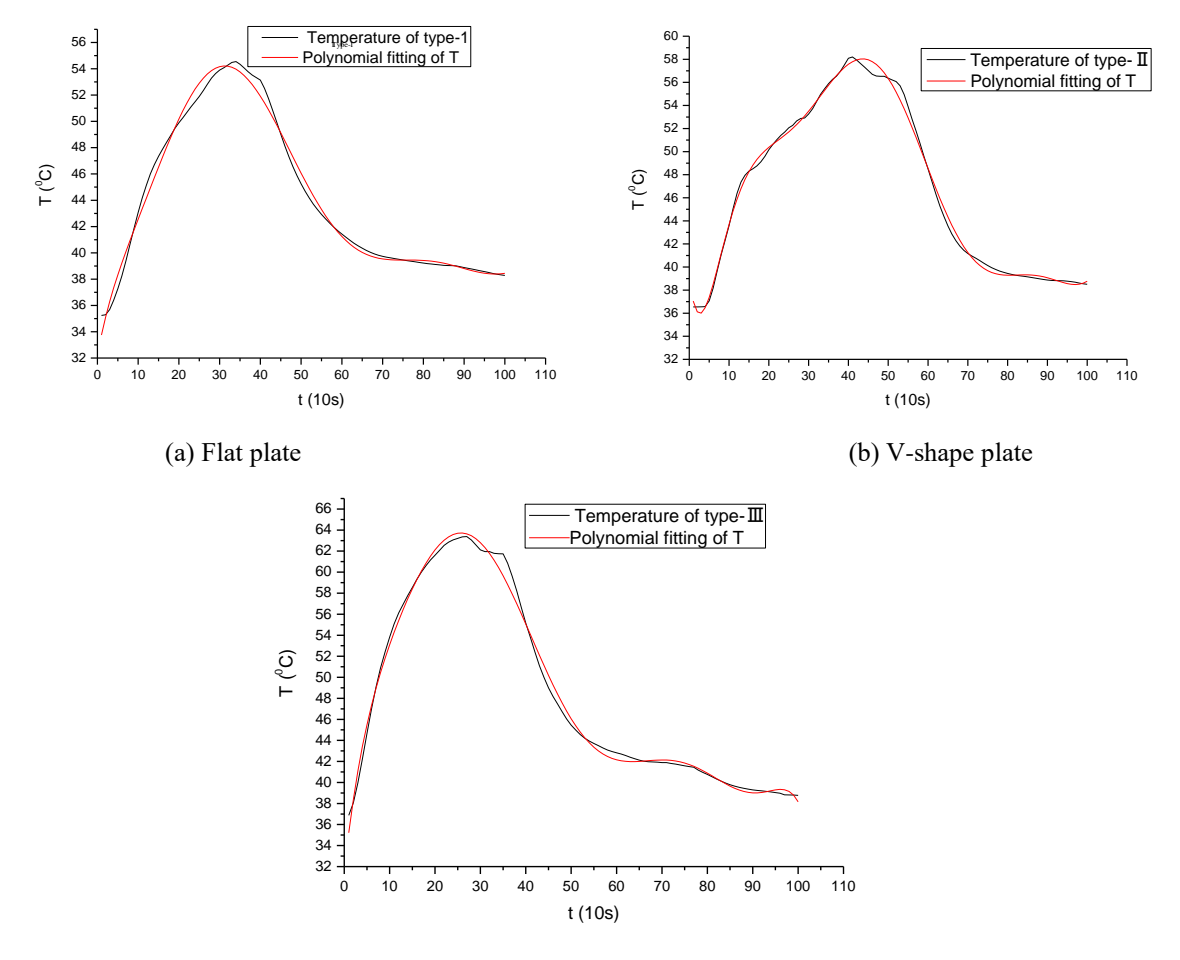
Figure 6 Light intensity distribution of different absorbers

Three kinds of the absorber plates were tested under the same condition, and temperature curves of the absorber plates with time are displayed in Figure 7. From Figure 7, it can be seen that the heating process takes a short time, while the cooling process takes a long time. Research also suggests that the temperature difference of Type-III is the highest and gets its peak in a comparatively short of time.

The comparison of absorption rates between experimental and simulated collector plates of different shapes is shown in table 2. From table 2, It can be seen that type-III has the highest absorption rate, followed by type-II and type-I. That is to say, the sinusoidal absorption plate has the highest absorption rate, while the flat plate has the lowest absorption rate. This is because when light shines on type-I, it can only reflect and absorb once, while when the light shines on type-II and type-III, it can reflect and absorb multiple times. This helps to enhance the optical efficiency of solar energy. The experimental value is less than the simulation value, the main reason is that there is energy loss in the actual operation.

Volume 18, No. 3, 2024

ISSN: 1750-9548



(c) Sinusoidal-corrugated plate

Figure 7 Temperature curve of absorber plates with time

Table 2 Comparison of absorption rates of three plates

Diata tuma	T_0	T_{max}	ΔΤ	Absorption	rate
Plate type	(°C)	(°C)	(°C)	Experimental value	Analog value
Type-I	35.68	54.54	18.86	0.8163	0.8366
Type- II	36.57	58.20	21.63	0.8790	0.9157
Type-III	36.87	63.39	26.52	0.9043	0.9445

Figure 8 shows the comparison of efficiency of solar air collectors with different structures under different air flow rates. From the Figure 8, it can be seen that the efficiency of the three types of collectors is the highest when the air flow rate is 80 m³/h, and the heat transfer efficiency of the collector is the lowest when the air flow rate is 40 m³/h. That is to say, the efficiency of air collectors improves with the enhance of flow rate. The main reason is that as the flow rate increases, the air flow rate increases, and the surface convective heat transfer coefficient enhances. The heat exchange between the air and the collector plate is more complete, and the heat carried away is also more, resulting in a decrease in temperature on the collector plate, a corresponding reduction in heat loss, and an increase in efficiency. When the flow rate decreases, the air flow rate decreases, the surface convective heat transfer coefficient decreases, and the heat transfer is insufficient, resulting in an enhancement in the temperature of the collector plate, corresponding heat loss increases, and efficiency also decreases.

Volume 18, No. 3, 2024

ISSN: 1750-9548

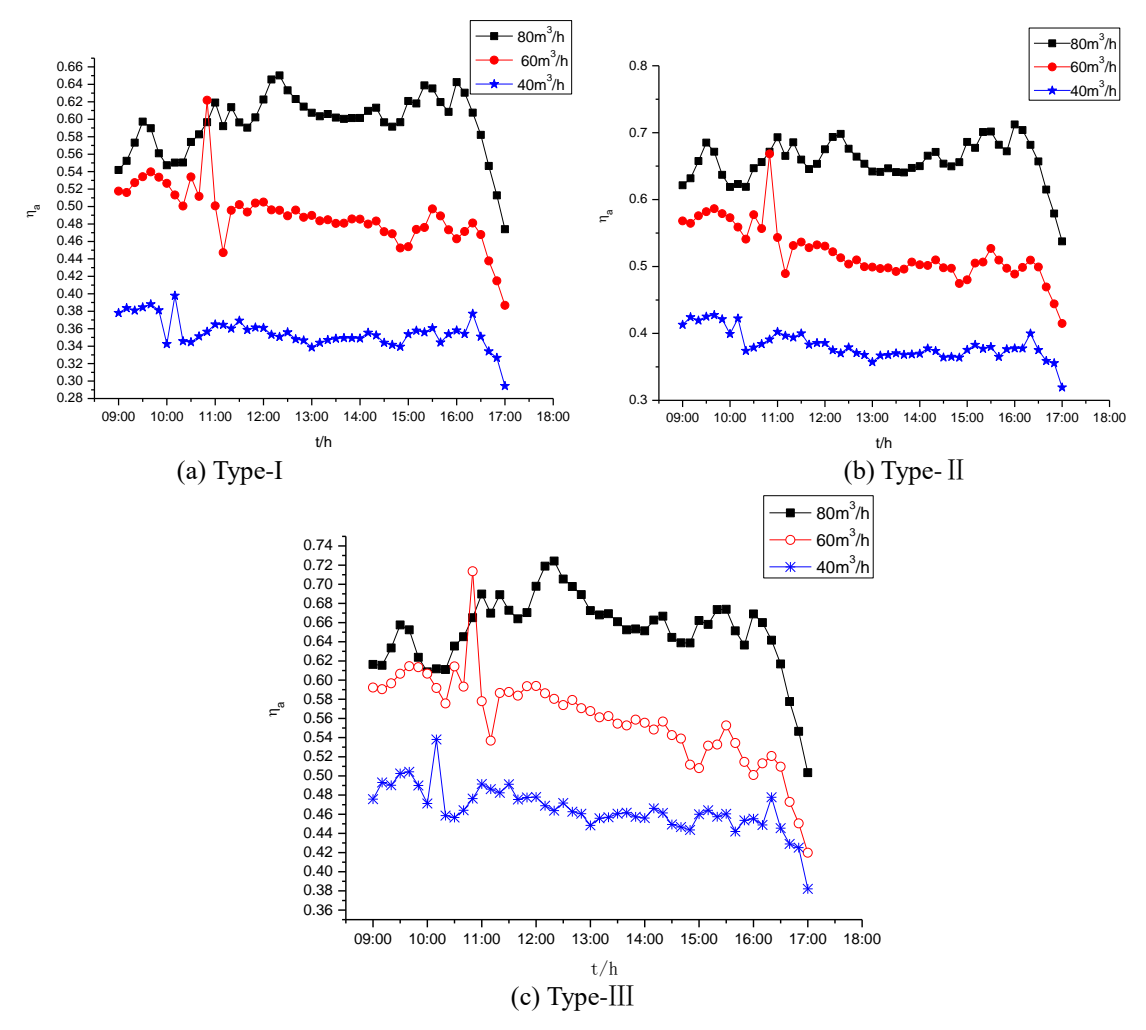


Figure 8 Efficiency curves of solar air collectors with different structure and airflow

Table 3 shows the comparison of performance parameters of collectors under different flow rates. From the table, it can be seen that the efficiency increases with the increase of flow rate, while the temperature of the collector plate and the temperature rise of the air decrease with the increase of flow rate. Under the same external environment, the air temperature rise and efficiency of Type III are the highest among the three types.

Date	$Q / m^3 \cdot h^{-1}$	Ambient Temperature/°C	Solar irradiance/W·m ⁻²	Туре	Temperature of plate/o	$C \begin{vmatrix} \Delta T \\ /^{\circ}C \end{vmatrix}$	$\eta_{\rm a}$ /%
03/09 80				Type-I	96.39	28.17	59.56
	31.089	731.157	Type- II	73.76	29.19	62.76	
				Type-III	52.01	29.42	65.08
05/09 60	33.767	713.087	Type-I	101.29	30.13	49.02	
			Type- II	76.49	30.18	52.02	
			Type-III	55.21	32.76	55.96	
29/08 40			Type-I	100.67	32.66	35.52	
	40	32.924	709.337	Type- II	76.84	33.06	38.17
				Type-III	57.08	40.43	46.50

Table 3. Comparison of collector parameters with different structures and airflow

5. Conclusions

Detailed analysis and experimental research were conducted on the absorption rates of absorption plates with different surface shapes. Through experimental research and simulation of the optical path of three types of absorption plates, it can be concluded that when light is irradiated on a flat absorption plate, light absorption and

reflection only occur once, while when light is irradiated on a V-shaped plate and a sine wave pattern plate, it occurs at least twice. The results indicate that under the same external environment, type-III has the highest air temperature rise and efficiency among the three types. The absorptivity of type-III is 10.78 % higher than that of type-I, so the shape change of the absorption plate can allow light to reflect and absorb multiple times, thereby improving its absorption rate

References

- [1] Yemeli Wenceslas Koholé, Fodoup Cyrille Vincelas Fohagui & Ghislain Tchuen. Flat-Plate Solar Collector Thermal Performance and Optimal Operation Mode by Exergy Analysis and Numerical Simulation. Arabian Journal for Science and Engineering volume 2021, vol. 46, pp. 1877-1897.
- [2] Kumar R., Sharma A, Goel V. An experimental investigation of new roughness patterns (dimples with alternative protrusions) for the performance enhancement of solar air heater. Renewable Energy 2023, vol. 211, pp: 964-974.
- [3] Varun Goel, V.S. Hans, et al. A comprehensive study on the progressive development and applications of solar air heaters. Solar Energy 2021, vol. 229, pp: 112-147.
- [4] Aman S., Ranjit S., Brij B. Review on Dimpled and Protruded Roughness Geometries used in the Duct of Solar Air Heaters. International Journal of Advance in Science and Engineering 2017, vol. 06, pp: 679-686.
- [5] Anil Kumar, Mamta Sharma, et al. A review on exergy analysis of solar parabolic collectors. Solar Energy 2020, vol.197, pp: 411-432.
- [6] Navneet A., Varun G., Bengt S. Solar air heater performance enhancement with differently shaped miniature combined with dimple shaped roughness: CFD and experimental analysis. Solar Energy 2023, vol. 250, pp: 33-50.
- [7] Alok Dhaundiyal, Gedion H. Gebremichael & Divine Aisu. Comprehensive Analysis of Solar Dryer with a Natural Draught. Energy Sources 2023, vol. 45, pp. 3563-3583.
- [8] Selçuk Darici, Anil Kilic. Comparative study on the performances of solar air collectors with trapezoidal corrugated and flat absorber plates. Heat and Mass Transfer 2020, vol. 56, pp. 1833–1843.
- [9] Abdulmohsen O. Alsaiari, Ahamed Iqbal, et al. Ebrahim. Heat transmission and air flow friction in a solar air heater with a ribbed absorber plate: A computational study. Case Studies in Thermal Engineering, 2022, vol. 40, pp: 383-396.
- [10] Yan Jiang, Huan Zhang, et al. A comparative study on the performance of a novel triangular solar air collector with tilted transparent cover plate. Solar Energy 2021, Volume 227, pp: 224-235.
- [11] Hirofumi Hattori, Kosuke Hotta, Tomoya Houra. Characteristics and structures in thermally-stratified turbulent boundary layer with counter diffusion gradient phenomenon. International Journal of Heat and Fluid Flow 2014, vol.49, pp: 53-61.
- [12] Hüseyin Benli. Experimentally derived efficiency and exergy analysis of a new solar air heater having different surface shapes. Renewable Energy, 2013, vol. 50, pp. 58-67.
- [13] Alsaleem S. M., Wright, L. M., Han J. C. Effect of the number of ribbed walls on the thermal performance in rectangular channels with 45-deg parallel or criss-cross ribs. International Journal of Heat and Mass Transfer 2023, vol. 207, pp: 1143–1156.
- [14] Gargioni G. T., Zdanski P. S. B., VazJr M. Heat transfer enhancement in flow past triangular turbulence promoters in closed channels. Numerical Heat Transfer 2019, vol. 75, pp: 309–326.
- [15] Giovanni Tanda, Essam Nabil Ahmed, Alessandro Bottaro. Natural convection heat transfer from a ribbed vertical plate: Effect of rib size, pitch, and truncation. Experimental Thermal and Fluid Science 2023, vol. 145, pp: 590–560.
- [16] Wang C. S., Shen P. Y., Liou, T. M. Evaluation of porous rib and flow pulsation on microchannel thermal performance using a novel thermal lattice Boltzmann method. International Journal of Thermal Sciences 2022, vol. 172, pp: 31–40.
- [17] Mahfuzur Rahman, Md. Shafiqul Islam, Abid Hossain Khan. Numerical investigation and benchmarking of heat transfer and pressure loss characteristics with two-sided rib-roughened and two-sided heat supply in narrow rectangular channels. Thermal Science and Engineering Progress 2023, vol. 41, pp. 183–195.

International Journal of Multiphysics

Volume 18, No. 3, 2024

ISSN: 1750-9548

- [18] Hui Xiao, Zhimin Dong, et al. Heat transfer performance and flow characteristics of solar air heaters with inclined trapezoidal vortex generators. Applied Thermal Engineering 2020, vol. 179, PP: 83–93.
- [19] Kasperski J., Magdalena N. Investigation of thermo-hydraulic performance of concentrated solar air-heater with internal multiple-fin array. Applied Thermal Engineering 2013, vol. 58, PP: 411-419.
- [20] Kushagra S., Harishchandra T. Heat transfer and fluid flow analysis of artificially roughened solar air heater. Materialstoday: Proceedings 2022, vol. 56, pp:910-920.
- [21] Li Shuilian, Meng Xiangrui. Effect of Buoyancy on the Perfomance of Solar Air Collectors with Different Structures. Applied Solar Energy, 2018, Vol. 54, No. 1, pp: 23–31.
- [22] Les Kirkup. Experimental Methods for Science and Engineering Students: An Introduction to the Analysis and Presentation of Data. Cambridge University Press 2019.